Synoptic Meteorology II: Introduction to Isentropic Potential Vorticity

Readings: Sections 4.1, 4.2, and 4.3.1 of *Midlatitude Synoptic Meteorology*.

The Relationship Between Relative Vorticity and Static Stability

To date, we have typically considered relative vorticity (a kinematic field) separately from static stability (a thermodynamic field). However, the two quantities are inextricably linked through the thermal wind relationship.

Let us consider a vertically localized maximum of relative vorticity, which is approximately equal to the geostrophic relative vorticity. A vertical cross-section through this feature along an east-west axis indicates northerly flow to the west and southerly flow to the east, each of which are maximized on the isobaric surface of the relative vorticity maximum (Fig. 1). To the west, v (or v_g) is less negative above and below the isobaric level of the relative-vorticity maximum; thus, the change in v with height is negative below and positive above this isobaric level. To the east, v is less positive above and below the isobaric level of the relative-vorticity maximum; thus, the change in v with height is positive below and negative above this isobaric level.

The thermal wind is the vector difference in the wind – specifically, the geostrophic wind – between two isobaric levels. The meridional component of the thermal wind is expressed as:

$$v_T = v_g\left(p_1\right) - v_g\left(p_0\right) = \frac{R_d}{f}\frac{\partial \overline{T_v}}{\partial x}\ln\left(\frac{p_0}{p_1}\right) \qquad (1)$$

where $p_0 > p_1$ (i.e., p_0 closer to the surface). The thermal wind links the change in geostrophic wind with height – here manifest through our relative-vorticity maximum – to horizontal variability in the layer-mean virtual-temperature field.

In Fig. 1, v_T is negative below the level of the relative-vorticity maximum to the west and above the level of the relative-vorticity maximum to the east. Likewise, v_T is positive above the level of the relative-vorticity maximum to the west and below the level of the relative-vorticity maximum to the east. This is depicted in black text on Fig. 1.

As a result, from (1), $\frac{\partial \overline{T_v}}{\partial x} < 0$ below the level of the relative-vorticity maximum to the west and above the level of the relative-vorticity maximum to the east and that $\frac{\partial \overline{T_v}}{\partial x} > 0$ above the level of the relative-vorticity maximum to the west and below the level of the relative-vorticity maximum to the east. In other words, virtual-temperature is a local minimum below and a local maximum above the level of the relative-vorticity maximum. This is depicted in purple text in Fig. 1.

If we assume that virtual temperature on an isobaric surface is closely approximated by potential temperature, we can infer the structure of the isentropes across the relative-vorticity maximum. As potential temperature typically increases upward, a local potential-temperature minimum implies lower-valued isentropes bowing up and a local potential-temperature maximum implies higher-valued isentropes bowing down. This is depicted in gold on Fig. 1.

Finally, recall that static stability is defined as the partial derivative of potential temperature with respect to pressure. As can be inferred from Fig. 1, the magnitude of the static stability is largest at the level of the relative-vorticity maximum and is smaller to the west and east. Thus, *relative-vorticity maxima and static-stability maxima are inextricably linked (in geostrophic conditions) by thermal wind!*

Why do we care? Let us begin by deriving isentropic potential vorticity…

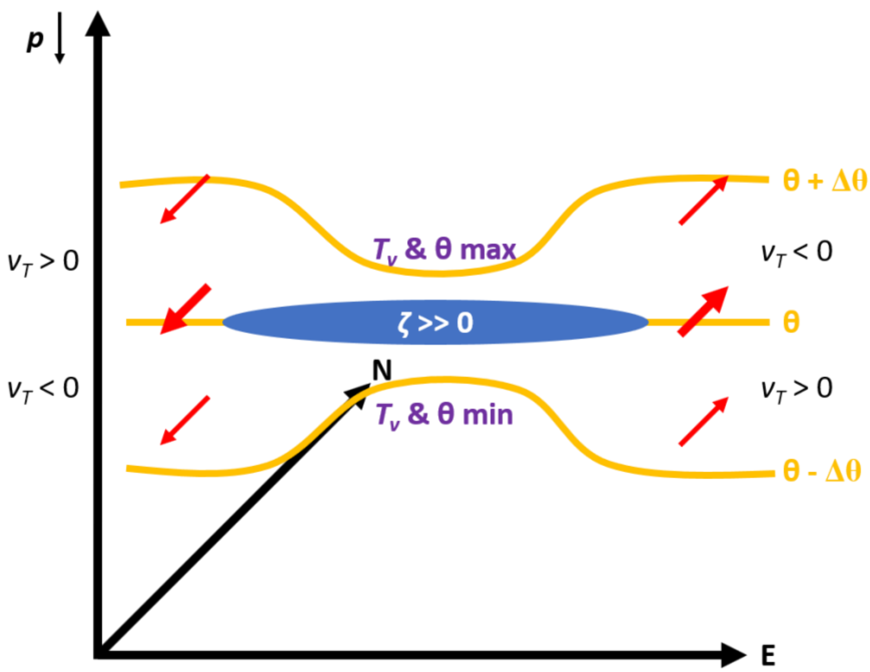

Figure 1. Vertical cross-section through a mid-tropospheric cyclonic relative-vorticity maximum (blue). The red arrows denote the associated meridional component of the geostrophic wind to its west and east; thicker arrows denote faster flow. The sign of the thermal wind in each layer to the west and east are given in black text and the relative magnitudes of T_v and θ are given in purple text. The isentrope configuration associated with the implied θ distribution is depicted by the gold contours. Please refer to the text above for more details.

Isentropic Potential Vorticity Derivation

We start by casting the horizontal momentum equation, neglecting friction and presented without derivation, into isentropic coordinates:

$$\frac{D\vec{\mathbf{v}}}{Dt} + f\hat{\mathbf{k}} \times \vec{\mathbf{v}} = -\nabla_{\theta} M \tag{2}$$

In (2), the subscript of θ implies that the gradient operator is applied on an isentropic surface. M is the Montgomery streamfunction.

On an isentropic surface, the total derivative in (2) takes the form:

$$\frac{D(\ )}{Dt} = \frac{\partial(\ )}{\partial t} + \vec{\mathbf{v}} \cdot \nabla_{\theta}(\ ) + \frac{d\theta}{dt}\frac{\partial(\ )}{\partial\theta} \tag{3}$$

where $d\theta/dt = \dot{\theta}$ is the diabatic heating rate, which we have sometimes also referred to as Q or dQ/dt. This term states that cross-isentropic flow occurs only when there is local diabatic heating ($d\theta/dt$ non-zero) contributing to potential temperature not being conserved following the motion. This implies vertical motion *between* isentropic surfaces. (Note, as we did in the last lecture, that vertical motion in isentropic coordinates can also be *along* an isentropic surface, or dry-adiabatic in nature.)

Note the similarity of (2) to its form in isobaric coordinates:

$$\frac{D\vec{\mathbf{v}}}{Dt} + f\hat{\mathbf{k}} \times \vec{\mathbf{v}} = -\nabla_{p} \Phi \tag{4}$$

In our last lecture, we demonstrated how the Montgomery streamfunction on an isentropic surface is an analog to the geopotential height on an isobaric surface. Therefore, it makes sense that the term on the right-hand side of the horizontal momentum equation in isentropic coordinates would be formulated based upon the Montgomery streamfunction rather than the geopotential height.

If we expand the total derivative in (2) by using (3), we obtain:

$$\frac{\partial\vec{\mathbf{v}}}{\partial t} + \vec{\mathbf{v}} \cdot \nabla_{\theta}\vec{\mathbf{v}} + \dot{\theta}\frac{\partial\vec{\mathbf{v}}}{\partial\theta} = -f\hat{\mathbf{k}} \times \vec{\mathbf{v}} - \nabla_{\theta} M \tag{5}$$

We now wish to obtain the vorticity equation for the isentropic coordinate system. Recall that the vorticity equation on an isobaric surface is obtained by taking $\hat{\mathbf{k}} \cdot \nabla \times$ of the horizontal momentum equation. In component form, this is equivalent to finding $\partial/\partial x$ of the *v*-momentum equation and subtracting $\partial/\partial y$ of the *u*-momentum equation from it. Doing so, we obtain:

$$\frac{\partial \zeta}{\partial t} + \vec{\mathbf{v}} \cdot \nabla_\theta (\zeta + f) + \dot{\theta} \frac{\partial \zeta}{\partial \theta} + (\zeta + f) \nabla_\theta \cdot \vec{\mathbf{v}} = \hat{\mathbf{k}} \cdot \frac{\partial \vec{\mathbf{v}}}{\partial \theta} \times \nabla_\theta \dot{\theta} \tag{6}$$

If we assume that potential temperature is conserved (purely dry-adiabatic flow), then the diabatic heating rate $\dot{\theta}$ is zero. Thus, the third term on the left-hand side of (6) and the only term on the right-hand side of (6) are both zero. Simplifying,

$$\frac{\partial \zeta}{\partial t} + \vec{\mathbf{v}} \cdot \nabla_\theta (\zeta + f) + (\zeta + f) \nabla_\theta \cdot \vec{\mathbf{v}} = 0 \tag{7}$$

The first term of (7) can alternately be written in terms of $\zeta + f$ because f does not change locally with time. As a result,

$$\frac{\partial (\zeta + f)}{\partial t} + \vec{\mathbf{v}} \cdot \nabla_\theta (\zeta + f) + (\zeta + f) \nabla_\theta \cdot \vec{\mathbf{v}} = 0 \tag{8}$$

We can write the continuity equation in isentropic coordinates as:

$$\frac{\partial}{\partial t}\left(\frac{\partial \theta}{\partial p}\right) - \frac{\partial \theta}{\partial p} \nabla_\theta \cdot \vec{\mathbf{v}} + \vec{\mathbf{v}} \cdot \nabla_\theta \left(\frac{\partial \theta}{\partial p}\right) = 0 \tag{9}$$

We now wish to combine (8) and (9) in such a way to eliminate the divergence term $\nabla_\theta \cdot \vec{\mathbf{v}}$ from the system of equations. To do so, we multiply (8) by $-g\partial\theta/\partial p$ and add to it (9) multiplied by -$g(\zeta+f)$. Doing so, we obtain:

$$g\left[\left(-\frac{\partial \theta}{\partial p}\right)\frac{\partial (\zeta + f)}{\partial t} + (\zeta + f)\frac{\partial}{\partial t}\left(-\frac{\partial \theta}{\partial p}\right) + (\zeta + f)\vec{\mathbf{v}} \cdot \nabla_\theta \left(-\frac{\partial \theta}{\partial p}\right) + \left(-\frac{\partial \theta}{\partial p}\right)\vec{\mathbf{v}} \cdot \nabla_\theta (\zeta + f)\right] = 0 \tag{10}$$

The inverse of the chain rule for partial derivatives may be used to combine the first two terms of (10) as well as the last two terms of (10). This allows us to write:

$$g\left[\frac{\partial}{\partial t}\left((\zeta + f)\left(-\frac{\partial \theta}{\partial p}\right)\right) + \vec{\mathbf{v}} \cdot \nabla_\theta \left((\zeta + f)\left(-\frac{\partial \theta}{\partial p}\right)\right)\right] = 0 \tag{11}$$

We define P, the *isentropic potential vorticity*, as:

$$P = -g\eta \frac{\partial \theta}{\partial p} \tag{12}$$

where $\eta = \zeta + f$, the absolute vorticity. Because g is a constant, we can take it into the partial derivatives of (11), allowing us to substitute (12) into (11) and obtain:

$$\frac{\partial P}{\partial t} + \vec{\mathbf{v}} \cdot \nabla_\theta P = 0 \Rightarrow \frac{DP}{Dt} = 0 \quad (13)$$

The Conservation of Isentropic Potential Vorticity

Equation (12) states that the isentropic potential vorticity is *conserved* following the motion along an isentropic surface (i.e., under dry-adiabatic conditions, such that diabatic heating is zero). Since we neglected friction in the horizontal momentum equation, isentropic potential vorticity is also conserved only under frictionless conditions (i.e., not near the surface). The non-conservation of isentropic potential vorticity following the motion along an isentropic surface thus can be used to infer where diabatic heating is occurring and/or where friction is important.

The isentropic potential vorticity P is a multiplicative function of two factors:

- Absolute vorticity η – a rotational constraint
- Static stability $-\partial\theta/\partial p$ – the vertical isentrope packing

Isentropic potential vorticity is a large positive value when cyclonic rotation is strong ($\eta > 0$) and static stability is large, representing isentropes that are tightly packed in the vertical ($-\partial\theta/\partial p >> 0$). ***Normally, $-\partial\theta/\partial p > 0$ (except near the surface with strong surface sensible heating, both conditions that are neglected in this formulation), such that $P < 0$ only occurs where $\eta < 0$***.

Localized maxima in isentropic potential vorticity are known as *positive potential vorticity anomalies*, whereas localized minima in isentropic potential vorticity are known as *negative potential vorticity anomalies*.

Since isentropic potential vorticity is conserved following the flow, if static stability or absolute vorticity change in value, the other must change in the opposite manner to keep the value of the isentropic potential vorticity constant.

- If the static stability increases, the absolute vorticity must decrease.
- If the static stability decreases, the absolute vorticity must increase.

These statements also hold true in the inverse; changes in absolute vorticity must be accompanied by changes in the static stability to keep the value of the isentropic potential vorticity constant. We can demonstrate this graphically via a vertical column of absolute vorticity between two isentropic surfaces, as depicted in Fig. 2.

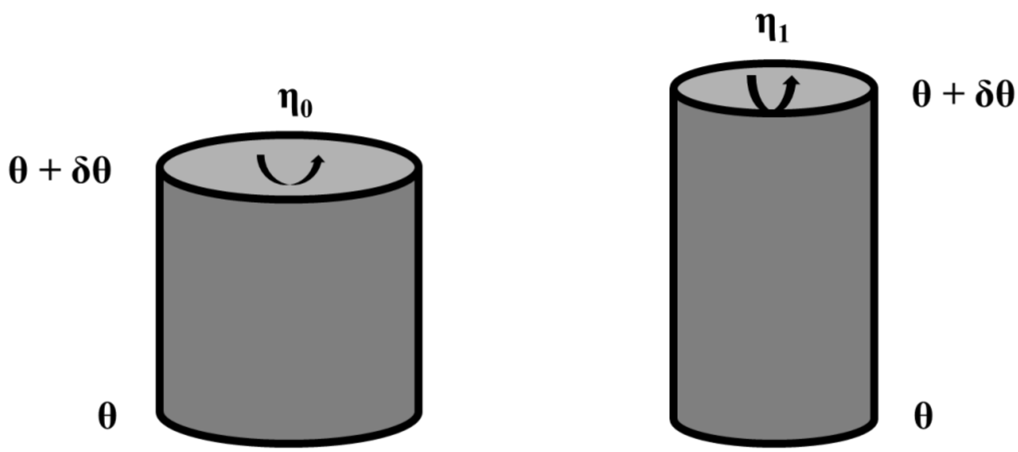

Figure 2. Schematic of a column of absolute vorticity between two isentropic surfaces at an initial (left) and a subsequent (right) time after the vorticity column has been stretched vertically.

The rotation rate at the initial time, as measured by the absolute vorticity, is given by η_0. The two isentropic surfaces θ and $\theta + \partial\theta$ are separated by a known increment $\partial\theta$. Likewise, the pressure difference between these two surfaces, ∂p is also known. If this column of vorticity is stretched vertically, the absolute vorticity increases. This can be shown using the vorticity equation, whether in its full or quasi-geostrophic form.

After stretching, the new absolute vorticity is given by η_1, where $\eta_1 > \eta_0$. The separation between the two isentropic surfaces, under dry-adiabatic conditions, remains $\partial\theta$. Because we vertically stretched the column, however, the difference in pressure between these two isentropic surfaces has increased. Thus, since ∂p is larger, $\partial\theta/\partial p$ is smaller, meaning that the static stability decreased to conserve isentropic potential vorticity.

Note that this relationship does not contradict the correspondence between relative-vorticity and static stability demonstrated earlier in this lecture: even after stretching, the rotation maximum is still associated with locally higher static stability as compared to its surroundings (which are not explicitly shown in Fig. 2 but can be inferred from the same thought experiment that went into obtaining Fig. 1).

On the synoptic-scale, isentropic potential vorticity anomalies evolve through a combination of translation, rotation, and deformation by the synoptic-scale flow. For these processes, isentropic potential vorticity is conserved following the motion. However, friction and diabatic processes can also impact isentropic potential vorticity. When these processes are important, isentropic potential vorticity is *not* conserved following the motion. We will examine this concept in greater detail in a later lecture.

Introducing the Dynamic Tropopause

The units of P are relatively complex:

$$P = \left(\frac{m}{s^2}\right)\left(\frac{1}{s}\right)\left(\frac{K}{Pa}\right) = \left(\frac{m}{s^2}\right)\left(\frac{1}{s}\right)\left(\frac{K\ m\ s^2}{kg}\right) = m^2\ K\ s^{-1}\ kg^{-1}$$

For typical midlatitude, synoptic-scale flow, $g \approx 10$ m s^{-2}, $\eta \approx f \approx 1 \times 10^{-4}$ s^{-1}, and $\partial\theta/\partial p \approx -10$ K per 100 hPa (or 10000 Pa). It should be noted, however, that the actual value of the static stability is typically less than this scale value except with strong temperature inversions. If we plug these values into (12), we obtain a characteristic value of $P = 1 \times 10^{-6}$ m^2 K s^{-1} kg^{-1}. For simplicity, we term this value to be equal to 1 PVU, where PVU defines *potential vorticity unit*.

In the troposphere, P is typically less than or equal to 1.5 PVU. Exceptions are typically confined to smaller-scale phenomena such as tropical cyclones with strong cyclonic rotation. In the stratosphere, where the static stability is very large as potential temperature rapidly increases with height, P is typically greater than 2 PVU. The tropopause is the transition region between the lower tropospheric values and higher stratospheric values of isentropic potential vorticity.

This gives rise to the construct of the *dynamic tropopause* (DT), which is commonly represented by the 1.5 PVU or 2 PVU surface. The DT is the representation of the tropopause by a surface of constant P. Just as the isentropic potential vorticity is conserved following the flow on an isentropic surface, the inverse must also be true: potential temperature is conserved following the flow on a surface of constant P. Consequently, where potential temperature changes following the flow on the DT, one can infer that diabatic processes (e.g., latent heat release) are ongoing and potentially important to the evolution of the synoptic-scale pattern.

Since potential temperature generally increases with height, analyses of potential temperature on the DT can be used to infer the relative height of the tropopause. Where potential temperature is relatively high on the DT, the tropopause itself is at a relatively high altitude, inferring an upper-tropospheric ridge. Where potential temperature is relatively low on the DT, the tropopause itself is at a relatively low altitude, inferring an upper-tropospheric trough.

This is demonstrated by Fig. 3. Relatively high potential temperature on the DT is found across the eastern United States and relatively low potential temperature on the DT is found across the western United States. The wind field is anticyclonically curved across the eastern United States whereas it is cyclonically curved across the western United States, in agreement with what we would expect given the theory above. As one might expect, the strongest winds on the DT are found in conjunction with the largest horizontal gradients of potential temperature along the DT.

We can confirm these insights by comparing Fig. 3 to Fig. 4. At 300 hPa, a trough is found across the western United States whereas a ridge is found across the eastern United States. At any given latitude, air temperatures are relatively cold near the trough and relatively warm near the ridge. Since pressure is inherently constant on an isobaric surface, this implies relatively low upper-tropospheric potential temperature in the western United States and relatively high upper-tropospheric potential temperature across the eastern United States. The strongest winds are found along the periphery of the trough and ridge, where the horizontal height and potential-temperature gradients are at their largest.

Before proceeding, it is worth stating a cautionary note. Air temperature typically increases – or at least remains constant – across the tropopause. As a result, air temperature in the heart of an upper-tropospheric trough on ***an isobaric surface intersecting the tropopause*** may appear warm compared to its surroundings at locations that are above the tropopause. Therefore, care must be taken when analyzing features on isobaric surfaces intersecting the tropopause. The same does not hold true on the DT, however, since it is defined by the tropopause (and thus does not cross it); low (high) potential temperature always corresponds to a lower (higher) tropopause height.

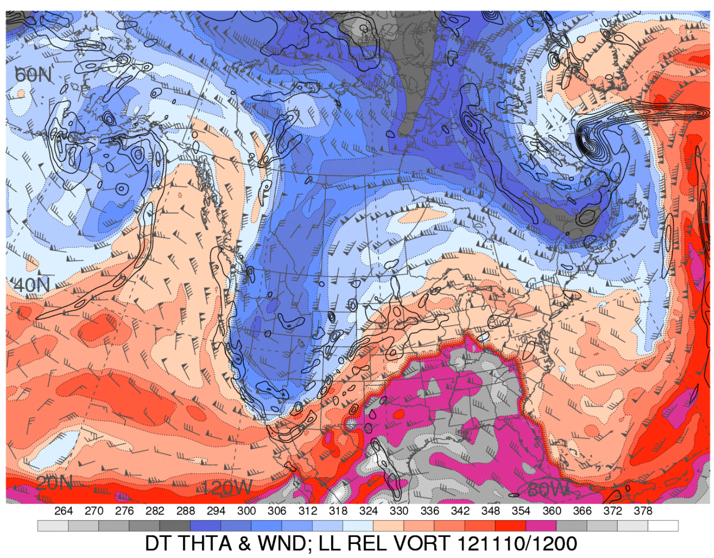

Figure 3. Potential temperature (shaded; units: K) and wind (barbs; half: 5 kt, full: 10 kt; pennant: 50 kt) on the dynamic tropopause, as represented by the 1.5 PVU surface, at 1200 UTC 10 November 2012. Also depicted is the 925-850 hPa layer mean relative vorticity (contours; every 5 x 10^{-5} s^{-1}). Image courtesy Heather Archambault.

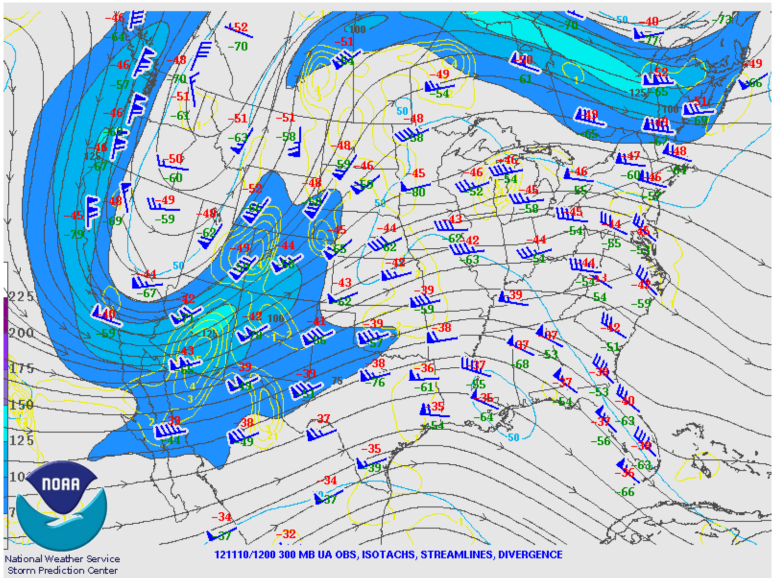

Figure 4. Streamlines (black contours), horizontal winds (shaded; units: kt), and upper air observations (barbs: wind in kt, red numbers: air temperature in °C, green numbers: dewpoint temperature in °C) at 1200 UTC 10 November 2012. Image courtesy Storm Prediction Center.

Potential Vorticity on Isobaric Surfaces

Note that P is conserved following the flow *only* on isentropic surfaces; it is *not* conserved on isobaric surfaces. Given that most meteorological data are obtained, displayed, and interpreted on isobaric surfaces, it is fair to ask whether a similar quantity is conserved on isobaric surfaces.

The *Ertel potential vorticity*, or EPV, is conserved following the full three-dimensional flow on isobaric surfaces if the flow is dry adiabatic and frictionless. EPV can be expressed as:

$$EPV = -g\left(f\hat{\mathbf{k}} + \nabla_3 \times \vec{\mathbf{v}}\right)\cdot \nabla_3 \theta \qquad (14)$$

In (14), subscripts of 3 refer to the gradient being evaluated in all three dimensions: x, y, and p.

If we complete the vector operations in (14) to expand the EPV into its components, we obtain:

$$EPV = -g\left[\left(\frac{\partial \omega}{\partial y} - \frac{\partial v}{\partial p}\right)\frac{\partial \theta}{\partial x} - \left(\frac{\partial \omega}{\partial x} - \frac{\partial u}{\partial p}\right)\frac{\partial \theta}{\partial y} + \eta\frac{\partial \theta}{\partial p}\right] \qquad (15)$$

If we presume that the horizontal vorticity – the terms involving ω and the partial derivatives of u and v with respect to p, representing rotation about the x and y axes – is small, we can simplify (15). This presumption is equivalent to stating the vertical motion and its horizontal gradients are relatively small on the synoptic-scale and that the troposphere is approximately barotropic such that horizontal wind speed and direction are nearly constant with height.

This simplified form of (15) is thus given by:

$$EPV \approx -g\eta \frac{\partial \theta}{\partial p} \qquad (16)$$

(16) is identical to (10), except applied on an isobaric surface and is explicitly an approximation. The basic interpretation of midlatitude, synoptic-scale weather phenomena is identical whether isentropic or Ertel potential vorticity are used. However, care should be taken to remember that *P* is conserved following the motion on isentropic surfaces, whereas EPV is conserved following the motion on isobaric surfaces. (Both are conserved only for frictionless, dry-adiabatic flow.)

Likewise, it should be reiterated that the EPV given in (16) is just that – an approximation. *For greatest accuracy*, *P* should be computed and interpreted exclusively on isentropic surfaces while the full, rather than approximate, EPV should be computed and interpreted exclusively on isobaric surfaces. Nevertheless, the form of potential vorticity given by the approximate EPV in (16) is that which is most often considered in synoptic-scale meteorology, largely because it is simpler to compute than its full form on isobaric surfaces and its counterpart on isentropic surfaces.

Applying Isentropic Potential Vorticity to Synoptic Analysis

Earlier, we stated that lower values of potential temperature on the DT imply lower tropopause heights and upper-tropospheric troughing. Meanwhile, higher values of potential temperature on the DT imply higher tropopause heights and upper-tropospheric ridging. This is demonstrated in Fig. 5. The DT is found at relatively low altitudes on relatively low isentropic surfaces near the poles and at relatively high altitudes and on relatively high isentropic surfaces near the Equator.

These concepts can be understood from thickness arguments. Averaged over the course of a year, incident solar radiation is greatest at the Equator and lowest at the poles. Correspondingly, the annually averaged, tropospheric-mean temperature is greatest at the Equator and lowest at the poles. This implies relatively low thicknesses at higher latitudes and relatively high thicknesses at lower latitudes. Consider the case where the lower surface is taken to be the ground, which is at a constant altitude, and the upper surface is taken to be the tropopause. Lower thicknesses thus imply a lower tropopause height near the poles, while higher thicknesses imply a higher tropopause height near the Equator.

Fig. 5 also demonstrates how one isentropic surface can be in the stratosphere at one location and in the troposphere at another. Take, for example, the 350 K isentropic surface. It is found between 200-250 hPa at nearly all latitudes, particularly in panel (a). In the tropics, this is in the troposphere, beneath the DT. However, the 350 K isentropic surface intersects the DT at around 30°N/30°S latitude, and at higher latitudes it is situated within the stratosphere.

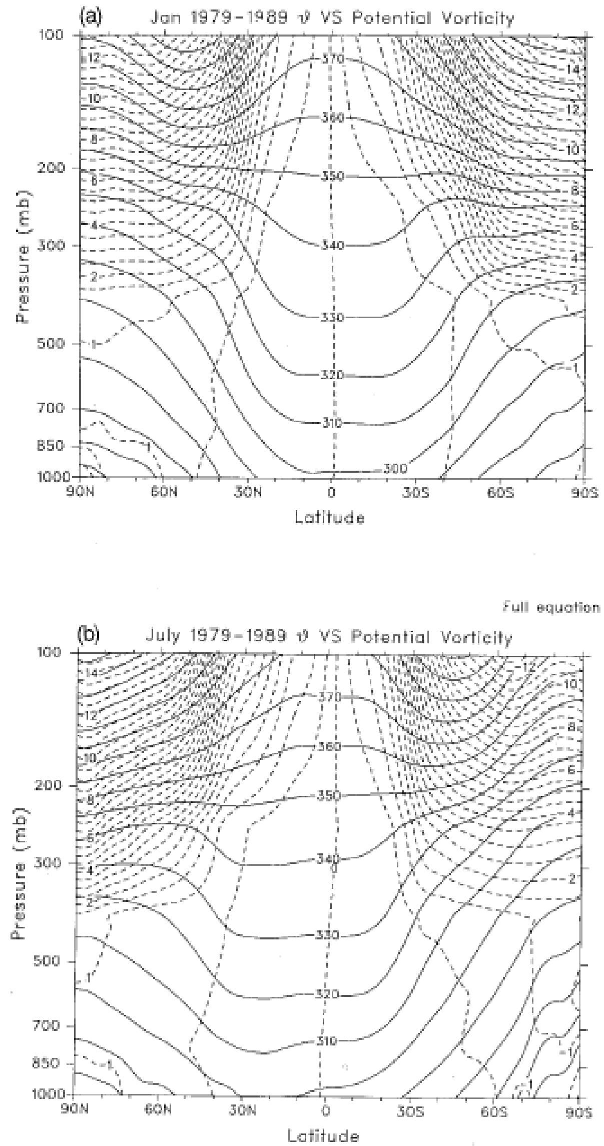

Figure 5. Vertical cross-sections of zonally averaged, climatological mean potential vorticity (dashed lines; units: PVU) and potential temperature (solid lines; units: K) for (a) January and (b) July. Reproduced from *Synoptic-Dynamic Meteorology in Midlatitudes* (Vol. II) by H. Bluestein, their Fig. 1.137.

In Figs. 3 and 4, we demonstrated the link between potential-temperature anomalies on the DT and troughs and ridges on upper-tropospheric isobaric charts. Now, we demonstrate the link between potential vorticity on an isentropic surface and troughs and ridges on upper-tropospheric isobaric charts. This is illustrated by Figs. 6 and 7. Equatorward extensions of the DT reflect upper- tropospheric troughs, the presence of cyclonically curved flow, and relatively cold temperatures. Poleward extensions of the DT reflect upper-tropospheric ridges, the presence of anticyclonically curved flow, and relatively warm temperatures.

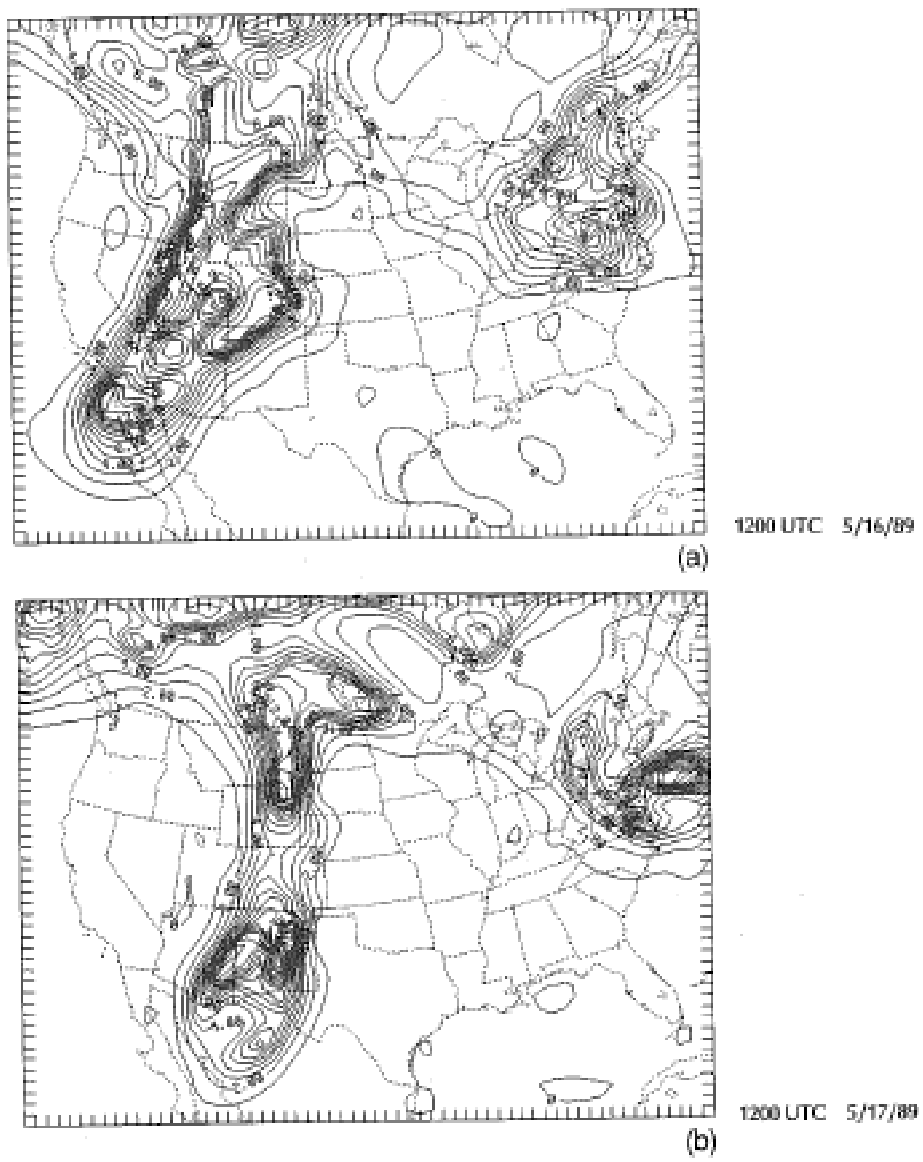

Figure 6. Isentropic potential vorticity (contours; every 1 PVU) on the 325 K isentropic surface valid at (a) 1200 UTC 16 May 1989 and (b) 1200 UTC 17 May 1989. Reproduced from *Synoptic-Dynamic Meteorology in Midlatitudes* (Vol. II) by H. Bluestein, their Fig. 1.138.

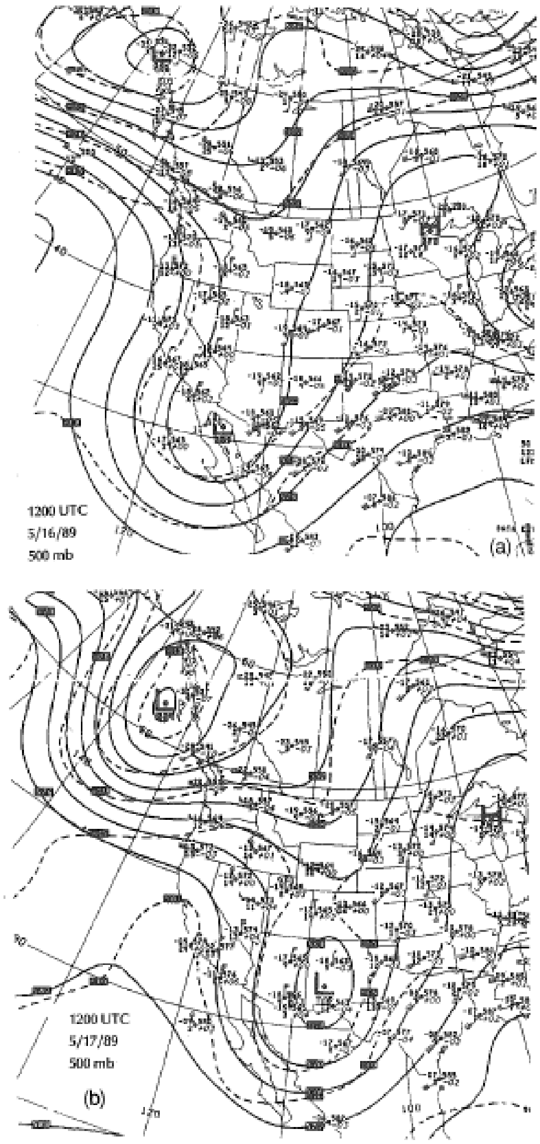

Figure 7. 500 hPa height (solid contours every 60 m), temperature (dashed contours every 5°C), and upper air observations (station plots of temperature in °C, dew point depression in °C, wind in kt, and height in dam) at (a) 1200 UTC 16 May 1989 and (b) 1200 UTC 17 May 1989. Reproduced from *Synoptic-Dynamic Meteorology in Midlatitudes* (Vol. II) by H. Bluestein, their Fig. 1.139.